Clinical Cancer Research

The Novel Bromodomain and Extraterminal Domain Inhibitor INCB054329 Induces Vulnerabilities in Myeloma Cells That Inform Rational Combination Strategies

Matthew C. Stubbs, Timothy C. Burn, Richard Sparks, Thomas Maduskuie, Sharon Diamond, Mark Rupar, Xiaoming Wen, Alla Volgina, Nina Zolotarjova, Paul Waeltz, Margaret Favata, Ravi Jalluri, Huiqing Liu, Xuesong Mike Liu, Jun Li, Robert Collins, Nikoo Falahatpisheh, Padmaja Polam, Darlise DiMatteo, Patricia Feldman, Valerie Dostalik, Pramod Thekkat, Christine Gardiner, Xin He, Yanlong Li, Maryanne Covington, Richard Wynn, Bruce Ruggeri, Swamy Yeleswaram, Chu-Biao Xue, Wenqing Yao, Andrew P. Combs, Reid Huber, Gregory Hollis, Peggy Scherle, and Phillip C.C. Liu

Abstract

Purpose: Bromodomain and extraterminal domain (BET) proteins regulate the expression of many cancer-associated genes and pathways; BET inhibitors have demonstrated activity in diverse models of hematologic and solid tumors. We report the preclinical characterization of INCB054329, a structurally distinct BET inhibitor that has been investigated in phase I clinical trials.

Experimental Design: We used multiple myeloma models to investigate vulnerabilities created by INCB054329 treatment that could inform rational combinations.

Results: In addition to c-MYC, INCB054329 decreased expression of oncogenes *FGFR3* and *NSD2/MMSET/WHSC1*, which are deregulated in t(4;14)-rearranged cell lines. The profound suppression of *FGFR3* sensitized the t(4;14)-positive cell line OPM-2 to combined treatment with a fibroblast growth factor receptor inhibitor *in vivo*. In addition, we show that BET inhibition across multiple myeloma cell lines resulted in suppressed interleukin (IL)-6 Janus kinase–signal transducers and activators of transcription (JAK–STAT) signaling. INCB054329 displaced binding of BRD4 to the promoter of IL6 receptor (IL6R) leading to reduced levels of IL6R and diminished signaling through STAT3. Combination with JAK inhibitors (ruxolitinib or itacitinib) further reduced JAK–STAT signaling and synergized to inhibit myeloma cell growth *in vitro* and *in vivo*. This combination potentiated tumor growth inhibition *in vivo*, even in the MM1.S model of myeloma that is not intrinsically sensitive to JAK inhibition alone.

Conclusions: Preclinical data reveal insights into vulnerabilities created in myeloma cells by BET protein inhibition and potential strategies that can be leveraged in clinical studies to enhance the activity of INCB054329.

Introduction

Bromodomain and extraterminal domain (BET) proteins comprise a family of four related proteins (BRD2, BRD3, BRD4, and BRDT), each harboring two tandem amino-terminal bromodomains (BD1 and BD2) that bind selectively to acetylated lysine residues. BET proteins regulate the expression of an array of genes by binding to highly acetylated histone tails at the promoters and enhancers of target genes and by recruiting transcriptional complexes including the super-elongation complex and the protein transcriptional elongation complex B (1, 2). Association of BRD4 with chromatin is strongly enriched at large enhancer elements, called super-enhancers, which are frequently co-opted in tumor cells to drive expression of genes involved in cell proliferation, cell fate, and survival (3, 4). Correspondingly, reduction of BRD4 by siRNA in transformed cells inhibits cell-cycle progression, due to G_1 arrest (5, 6).

The small-molecule inhibitors, JQ-1 and iBET, that block BET binding to chromatin showed therapeutic potential against both solid and hematologic tumor models, in part, through suppression of oncogenes such as *c-MYC* (7–9). In addition, BRD2, BRD3, and BRD4 have been shown to control the inflammatory response in models of acute inflammation by regulating the expression of proinflammatory modulators such as interleukin (IL)-6 and tumor necrosis factor (TNF)α (8, 10). Tumor-associated inflammation is a hallmark of cancer, and elevated levels of proinflammatory proteins, including IL6, have been shown to promote multiple aspects of tumorigenesis. Thus, antitumor activity of BET inhibitors may result from modulation of inflammation in addition to direct effects on the tumor cell.

Incyte Corporation, Wilmington, Delaware.

Note: Supplementary data for this article are available at Clinical Cancer Research Online (http://clincancerres.aacrjournals.org/).

Corresponding Authors: Matthew C. Stubbs, Incyte Corporation, 1801 Augustine Cut-off, Wilmington, DE 19803. Phone: 302-498-5716; E-mail: mstubbs@incyte.com; and Phillip C.C. Liu, pliu@incyte.com

doi: 10.1158/1078-0432.CCR-18-0098

Translational Relevance

Here, we describe INCB054329, a structurally distinct bromodomain and extraterminal domain (BET) inhibitor that is potent in several preclinical models of B-cell malignancies and is currently in phase I trials. The key to successful utilization of BET inhibitors may lie in their ability to enhance the efficacy of other targeted therapies. Here, we demonstrate that INCB054329 can be rationally combined with inhibitors of signaling pathways in models of multiple myeloma, in which pathway components are transcriptionally regulated by BET proteins. We report that INCB054329 sensitizes myeloma cells both *in vitro* and *in vivo* to clinical Janus kinase inhibitors, such as ruxolitinib, by reducing interleukin-6 receptor expression, and to the phase II fibroblast growth factor receptor (FGFR) inhibitor INCB054828 in subsets of t(4;14) translocated myelomas with high FGFR3 expression. These findings may lead to improved stratification strategies for patients receiving BET inhibitors, such as those with activation of BET-regulated kinase pathways.

Multiple myeloma is a progressive cancer of malignant plasma cells that initiates from genetic lesions including copy-number alterations and chromosomal translocations resulting from immunoglobulin switch recombination (11, 12). Juxtaposition of the immunoglobulin heavy-chain (IgH) enhancers to oncogenes, such as *FGFR3*/*MMSET* or *CCND1* in t(4;14) and t(11;14), respectively, occurs as early initiating events in approximately 25% of cases (13). Progression corresponds to the accumulation of secondary genetic and epigenetic alterations including the deregulation of *c-MYC* by various chromosomal rearrangements (14, 15). The survival and proliferation of both normal and malignant plasma cells are critically dependent upon the interaction with a variety of cells in the bone marrow microenvironment, including stromal, vascular, bone, and immune cells (16). Interactions among these cells are mediated by cytokine receptors, which include IL6, insulin-like growth factor-1, basic fibroblast growth factor, and various other chemokines and cytokines.

We present the preclinical characterization of a novel, phase I BET inhibitor, INCB054329. Our data demonstrate that, in addition to *c-MYC*, other putative oncogenes such as FGFR3 and pathways including JAK–STAT are strongly affected by BET inhibition in models of myeloma, thereby creating vulnerabilities that can be exploited with targeted agents. These results provide a strategy for potential selection of rational combinations with BET inhibitors.

Materials and Methods

Cell lines and reagents

All cell lines except INA-6 were purchased from ATCC, DSMZ, or the Japanese Collection of Research Bioresources Cell Bank and were acquired between 2003 and 2013. INA-6 cells were a gift from Dr. Renate Burger (University Hospital Schleswig-Holstein, Kiel, Germany). All cell lines were confirmed to be negative for *mycoplasma* (Bionique Testing Laboratories, Inc.), and cell lines used for *in vivo* testing were authenticated by short tandem repeat analysis between 2013 and 2017. INCB054329, INCB054828, ruxolitinib, itacitinib, and JQ-1 were synthesized at Incyte Corporation.

Bromodomain-binding assays

The binding of INCB054329 to BET bromodomains BRD4-BD1 and BRD4-BD2, BRD3-BD1 and BRD3-BD2, BRD2-BD1 and BRD2-BD2, and BRDT-BD1 was assessed using the AlphaScreen assay (PerkinElmer). A fluorescence polarization assay was used to measure binding to the BRDT-BD2. Binding to non-BET bromodomains was assessed using the BROMO*scan* assay at a fixed concentration of 3 μmol/L of INCB054329 (DiscoverX).

Gene-expression analysis

Gene-expression analysis was performed using Affymetrix Human Genome U133 PLUS 2.0 microarrays with data being analyzed using OmicSoft's Array Studio software (OmicSoft Corporation) and gene set enrichment analysis (GSEA; refs. 17, 18). Chromatin immunoprecipitation (ChIP) sequencing was performed as described (19), with mapped reads being visualized in Array Studio.

Chromatin immunoprecipitation

Chromatin was isolated from cell lines using the SimpleChIP Enzymatic ChIP kit (Cell Signaling Technology). The antibodies used for ChIP were anti-BRD4 (Bethyl Laboratories; A301-985) and anti-Histone H3-acetyl K27 (Abcam; ab4729). Analyses of the IgH enhancers and the c-*MYC* transcriptional start site (TSS) were performed using published primer-probe sets (19). The forward and reverse primers for the negative control region of FGFR3 are 5′-GCGCTAACACCACCGACAA and 5′-GAGTGATGAGAAAACCCAATAGAATTG with the probe sequence 5′-AGCTAGAGGTTCTCTCCTTGCACAACGTCA. The primer and probe sequence for IL6 receptor alpha (IL6Rα) are 5′-GCGCGAGTTCCTCAAATGTT and 5′-TCCCACTCGCACATGACTCA with the probe sequence CCTGCGTTGCCAGGACCGTCC. These data are expressed as fold enrichment (2E[-ΔΔCt[ChIP/nonimmune control]) and normalized to the input (2% of the dimethyl sulfoxide [DMSO] sample).

Western blotting and ELISA

All antibodies were purchased from commercial sources as follows: antibodies against phosphorylated signal transducers and activators of transcription 3 (pSTAT3; pY705), STAT3, c-MYC, PIM2, phosphorylated fibroblast growth factor substrate 2 (FRS2; pY436), GAPDH, and Actin were from Cell Signaling Technology; antibodies against WHSC1/MMSET were from Novus Biologicals; antibodies against p21 were from BD Biosciences, and antibodies against fibroblast growth factor receptor 3 (FGFR3), pFGFR3 (pY724), and FRS2 were from Abcam. The c-MYC ELISA kit was purchased from Cell Signaling Technology, and ELISA was performed per the manufacturer's protocol.

Cell viability assay

Cell viability assays were performed after 72 hours of incubation with a serial dilution of INCB054329 or 0.1% DMSO as control using the CellTiter-Glo ATP assay (Promega). All cell lines were tested with a minimum of three independent experiments, and data are reported as the mean ± standard deviation. To test dependence of the OPM-2 cells on FGFR3, gene editing by

CRISPR-Cas9 was performed using 3 gRNAs targeted to FGFR3 and a control gRNA targeting Green Fluorescent Protein (Cellecta Inc.). OPM-2-Cas9 cells were generated by infection of lentiviral Cas9, followed by selection with 5 μg/mL blasticidin for 1 week. OPM-2-Cas9 cells were infected with gRNAs for 2 days and then selected using 1 μg/mL puromycin for 3 days to eliminate uninfected cells. Edited cells were counted and seeded into 96 wells (3,000/well), and growth of the cells was measured over time as described. FGFR3 knockdown was confirmed by Western blotting. The gRNA sequences used for targeting GFP and FGFR3 are as follows: gGFP: AAGATCGAGTGCCGCATCAC; gFGFR3-1: GGGGACGGAGCAGCGCGTCG; gFGFR3-1: GGGAGATGACGAAGACGGGG; gFGFR3-1: GCTGCCGGCCAACCAGACGG.

Human T-cell assays

T cells were separated from human peripheral blood mononuclear cells of healthy adults by elutriation and treated with phytohemagglutinin (PHA) for 3 days to induce cell-surface expression of IL2 receptors. The PHA-activated and phosphate-buffered saline-washed T cells were grown in the presence of 100 U/mL of IL2 and different concentrations of INCB054329 for 3 days. Proliferation analysis was performed using CellTiter-Glo Reagent as described above.

Cell-cycle analysis

Cell-cycle distribution was determined using propidium iodide staining and analyzed by flow cytometry according to established protocols. The kinetic parameters of the cell cycle (G_1, S, G_2+M) and the coefficient of variance of G_1 peak from 50,000 events were computed using the Cflow Plus software (BD Biosciences).

Analysis of apoptosis

Apoptosis was determined using Annexin V–propidium iodide staining of cells treated with INCB054329 or DMSO vehicle according to standard procedures, and data from 10,000 events were analyzed by CflowPlus Software using an Accuri C6 cytometer (BD Biosciences).

In vivo experiments

All experiments involving mice were performed under the guidelines and regulations of the Institutional Animal Care and Use Committee of Incyte Corporation. CB17/Icr-Prkdc scid/IcrIco Crl (severe combined immunodeficiency [SCID]) and Nu/Nu (nude) mice were purchased from Charles River Laboratories.

For the administration by oral gavage, all Incyte compounds were first reconstituted in *N*,*N*-dimethylacetamide (DMAC; Sigma-Aldrich) and then diluted in a 0.5% methylcellulose (Sigma-Aldrich) solution for a final concentration of 5% DMAC.

For xenograft studies, 10^7 cells were resuspended in Matrigel (BD Biosciences; KMS-12-BM and MM1.S) or resuspended as brei (INA-6) and injected subcutaneously into the dorsal flanks of mice. Subcutaneous tumors were allowed to grow until they reached approximately 200 mm^3, at which point the mice were randomized into dosing groups. Tumors were measured at least twice weekly with electronic calipers. Tumor volumes were calculated using the following formula: volume = (length × $width^2$)/2, where width was the smaller dimension. Body weights were also monitored.

Results

Discovery of a novel BET bromodomain inhibitor

A fragment to pharmacophore strategy was used to identify a novel fused tricyclic scaffold and subsequently led to the discovery of the candidate INCB054329 (Fig. 1A). The isoxazole moiety mimics the acetyl lysine group in the BRD4-BD1 pocket, and the pyridyl ring binds on the WPF shelf (Fig. 1B). In biochemical binding assays, INCB054329 potently inhibited the binding of tetra-acetylated histone H4 peptide to BRD2,

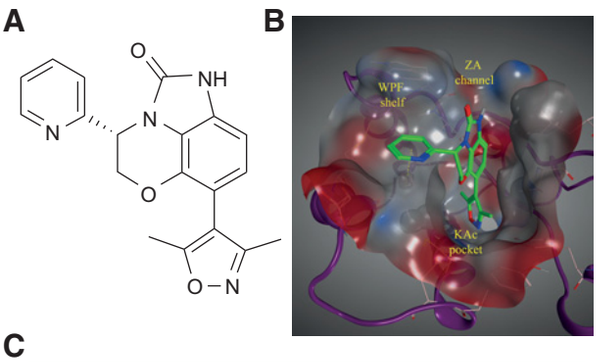

C

Bromodomain	IC_{50}, mean ± SD (nmol/L)
BRD2-BD1	44 ± 16
BRD2-BD2	5 ± 1
BRD3-BD1	9 ± 2
BRD3-BD2	1 ± 0.4
BRD4-BD1	28 ± 7
BRD4-BD2	3 ± 1
BRDT-BD1	119 ± 68
BRDT-BD2	63 ± 8

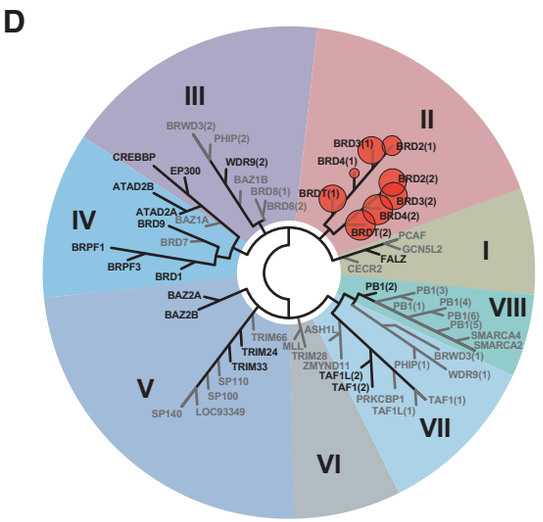

Figure 1.

Structure and characterization of the novel BET inhibitor INCB054329. **A,** Structure of INCB054329. **B,** Model of the interaction of INCB054329 with the acetyl lysine binding pocket of BRD4-BD1. **C,** Inhibition of tetra-acetylated histone H4 peptide binding to BRD2, BRD3, BRD4, and BRDT by INCB054329 in biochemical assays. **D,** INCB054329 is selective for the BET subfamily.

BRD3, and BRD4, with modest selectivity for BRDT-BD1 and BRDT-BD2 (Fig. 1C). A screen against 16 non-BET bromodomains showed no significant inhibitory activity at 3 μmol/L (Fig. 1D).

INCB054329 exhibits broad antiproliferative activity against hematologic cancer cell lines and antagonizes c-MYC expression *in vitro* and *in vivo*

The antiproliferative activity of INCB054329 was profiled against a panel of 32 hematologic cancer cell lines derived from acute myeloid leukemia, non-Hodgkin lymphoma, and multiple myeloma (Fig. 2A). The median 50% growth inhibition (GI_{50}) value was 152 nmol/L (range, 26–5,000 nmol/L), and inhibitory activity was observed across all histologies (Supplementary Table S1). In contrast to tumor cell lines, the GI_{50} value against T cells isolated from non-diseased donors stimulated *ex vivo* with IL2 was 2.435 μmol/L. Growth inhibition correlated with a concentration-dependent accumulation of cells in the G_1 phase of the cell cycle (Fig. 2B). An increase in apoptosis was also observed in four of five myeloma cell lines at 1,000 nmol/L, and significant increases were observed from 100 nmol/L in INA-6 cells (Fig. 2C). Consistent with published experiments (19), ChIP of BRD4 showed enriched binding at the IgH enhancers in MM1.S cells (Fig. 2D). Treatment with INCB054329 displaced BRD4 binding to the E2 3′ enhancer, similar to findings with the BET inhibitor JQ-1 (Supplementary Fig. S1; ref. 19). Concomitant with the abrogation of BRD4 binding, levels of c-*MYC* mRNA were rapidly suppressed, leading to a concentration-dependent decrease in c-MYC protein in multiple cell lines (Fig. 2E and F). Using c-MYC as a pharmacodynamic marker in tumor cells, we evaluated the pharmacokinetic–pharmacodynamic relationship after a single oral administration of INCB054329 in mice bearing subcutaneous xenografts of KMS-12-BM tumors. The KMS-12-BM cell line has been shown to have very high c-MYC protein levels (20) and is therefore amenable for pharmacokinetic/pharmacodynamic study. A concentration-dependent decrease was observed 3 hours after dose with an *in vivo* half-maximal inhibitory concentration (IC_{50}) of 66 nmol/L and a 90% inhibitory concentration (IC_{90}) of approximately 400 nmol/L (Fig. 2G). INCB054329 exhibited high clearance in mice resulting in a short half-life (Supplementary Fig. S2A); therefore, twice-daily (b.i.d.) dosing was used in efficacy studies. At exposures that effectively suppressed c-MYC, INCB054329 was found to be efficacious and well tolerated in both the KMS-12-BM and MM1.S xenograft models (Supplementary Fig. S2B and S2C).

INCB054329 displaces binding of BRD4 from enhancers driving oncogenes in models of t(4;14) myeloma

The t(4;14) translocation involves a balanced rearrangement of the IgH locus on chromosome 14, with chromosome 4 leading to deregulation of two potential oncogenes *FGFR3* (encoding a receptor tyrosine kinase) and *NSD2/MMSET/WHSC1* (encoding a DNA methyl transferase; Fig. 3A; ref. 13). To assess whether both translocation partners are regulated by BRD4, ChIP-PCR was performed on both the Eμ and E2 enhancers associated with the IgH locus. BRD4 binds to both elements in two t(4;14)-positive cell lines OPM-2 and KMS-11, with higher normalized levels at the E2 enhancer. Treatment with 500 nmol/L INCB054329 reduced BRD4 association with the E2 and Eμ enhancers to 8% and 29% of the DMSO control samples, respectively, in OPM-2 cells, while only BRD4 binding to E2 was reduced (18% of control) in the KMS-11 cells (Fig. 3B; Supplementary Fig. S1). Steady-state mRNA levels of FGFR3 were reduced to nearly background in the OPM-2 cells similar to c-MYC, while mRNA levels of NSD2 were decreased approximately 50% (Fig. 3C). FGFR3 protein levels were also suppressed to near background levels (1% of DMSO) at a concentration of 250 nmol/L (approximately twice the IC_{50}), whereas NSD2/MMSET protein was maximally reduced by 50% at 24 hours (Fig. 3D).

In a subcutaneous xenograft model of OPM-2 tumors, oral administration of INCB054329 resulted in a dose-dependent suppression of tumor growth and was well tolerated as assessed by body-weight measurements (Fig. 3E). The strong suppression of *FGFR3* suggested that greater inhibition of tumor growth could be achieved in combination with FGFR targeting. INCB054828 is a selective kinase inhibitor of the FGFR 1, 2, and 3 and is currently being tested in phase I/II trials of solid and hematologic cancers (NCT02393248 and NCT03011372). INCB054828 inhibited OPM-2 cell proliferation (GI_{50}, 97 nmol/L) similar to deletion of FGFR3, indicating at least partial dependence of these cells on FGFR signaling (Supplementary Fig. S3). *In vivo*, partial antitumor efficacy by INCB054828 was observed against OPM-2 xenografted tumors at its optimal dose of 0.3 mg/kg once daily (Fig. 3E). When combined with INCB054329, however, a significantly greater decrease in terminal tumor volume was achieved than by either compound alone ($P < 0.001$ by two-way ANOVA for combination versus each single agent). Strikingly, FGFR inhibition alone resulted in a feedback upregulation of FGFR3 that was completely abrogated in the combination group (Fig. 3F). Despite the increased FGFR3 levels in tumors from INCB054828-treated mice, signaling through FGFR3 is blunted by INCB054828 (as determined by pFGFR3 and pFRS2 levels), and slightly more so by the combination of INCB054828 and INCB054329. The combination also decreased levels of c-MYC and pSTAT3 and increased levels of p21 when compared with levels from single-agent–treated tumor samples.

Gene-expression profiling identifies key growth regulatory and inflammatory pathways as targets of INCB054329

To characterize the broader effects of BET inhibition on gene expression, two myeloma cell lines MM1.S and INA-6 were treated for 4 and 24 hours with INCB054329 and analyzed by gene-expression profiling (Supplementary Fig. S4A). Pathway analysis of differentially expressed genes was evaluated using two methods: MetaCore and GSEA. By MetaCore, a number of pathways related to growth, development, and inflammation were enriched (Fig. 4A). To explore molecular signatures in greater detail, the data were also analyzed by GSEA. c-MYC–dependent gene sets emerged among the top downregulated gene sets in both MM1.S and INA-6 cell lines (Fig. 4B; Supplementary Fig. S4B), and c-MYC was identified as the most significantly downregulated transcription factor network in MM1.S cells, recapitulating results with JQ-1 and other BET inhibitors (19, 21). In addition, the IL6 signature in myeloma was among the top pathways in both cell lines. In monocytes, BET inhibitors repressed production of IL6 (10), and INCB054329 also suppressed secretion of IL6 by immortalized, human stromal cell lines (Supplementary Fig. S5); however,

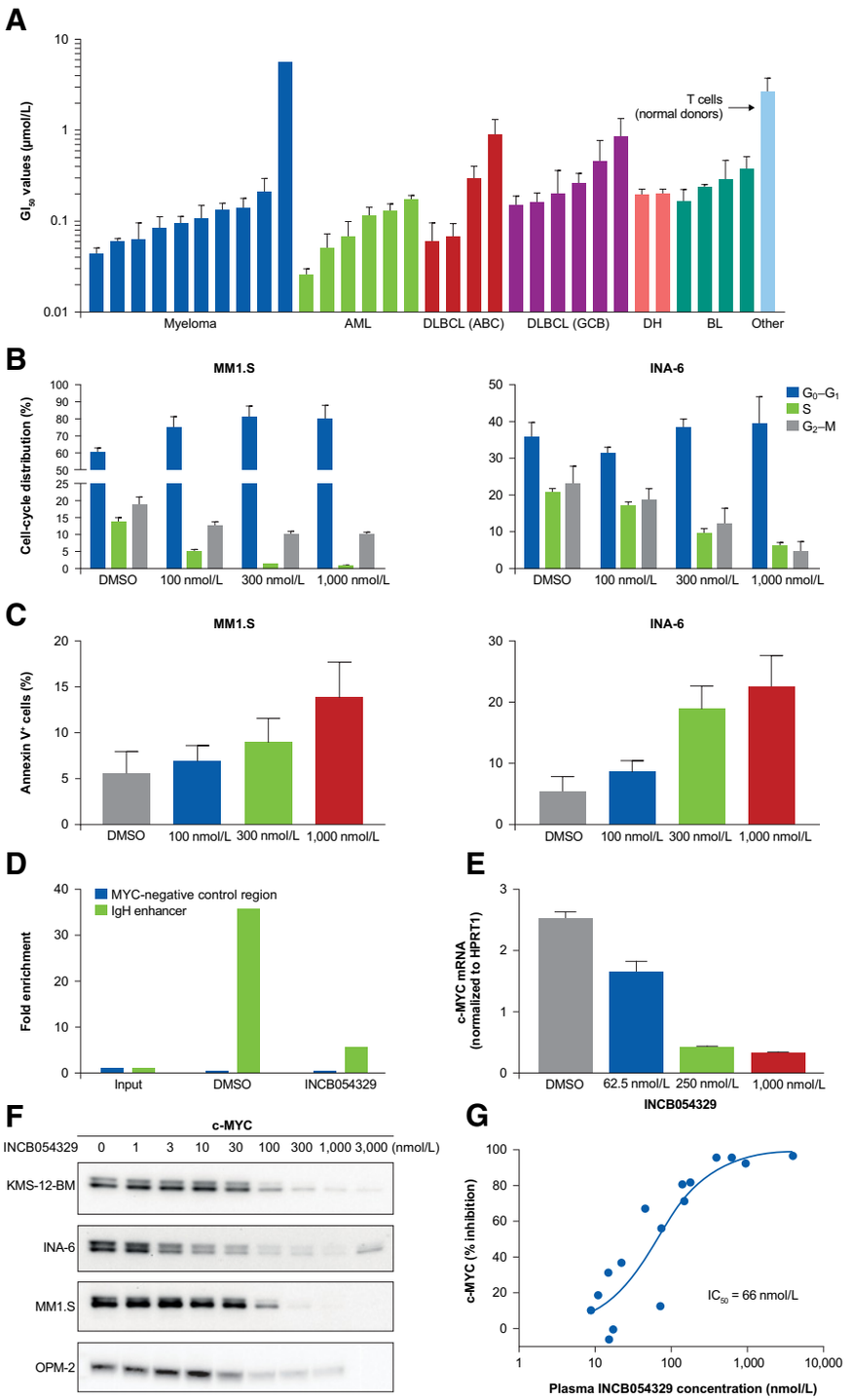

Figure 2.

INCB054329 has antiproliferative activity against hematologic cancer cell lines *in vitro* and suppresses expression of c-MYC *in vitro* and *in vivo*. **A,** Waterfall plot showing GI_{50} values against a panel of cell lines derived from hematologic cancers. T cells from normal donors stimulated *ex vivo* with IL2 were used as a normal comparator. All assays were run for 72 hours. Each GI_{50} value is the mean (±SD) for at least three independent experiments. **B,** Analysis of cell-cycle distribution by flow cytometry using propidium iodide staining for DNA content. MM1.S (left) or INA-6 (right) cells were treated with indicated concentrations of INCB054329 or DMSO (control) for 48 hours. Each bar shows the mean (±SD) for three independent experiments. **C,** Measurement of cellular apoptosis by Annexin V–propidium iodide staining after 48-hour incubation of MM1.S (left) or INA-6 (right) cells with INCB054329 or DMSO control. The mean increase over control (±SD) for three experiments is shown. **D,** Binding of BRD4 to the IgH enhancer E2 in MM1.S cells treated without or with 1,000 nmol/L INCB054329. **E,** Concentration-dependent reduction of steady-state c-MYC mRNA levels in MM1.S cells. **F,** Concentration-dependent suppression of c-MYC protein by INCB054329. Cells were treated with INCB054329 for 3 hours prior to Western blotting analysis with anti–c-MYC. **G,** *In vivo* pharmacokinetic–pharmacodynamic relationship. KMS-12-BM tumors were established in female Nu/Nu mice, and INCB054329 was administered orally at 0 (vehicle control), 3, 10, 30, or 100 mg/kg ($n = 5$ per group). At 3 hours after dose, peripheral blood and tumors were harvested. Plasma was analyzed by liquid chromatography–tandem mass spectrometry for INCB054329 concentration, and tumors were homogenized and analyzed for c-MYC protein levels using a c-MYC ELISA kit. The *in vivo* observed IC_{50} value was calculated to be 66 nmol/L. ABC, activated B-cell–like; AML, acute myelogenous leukemia; BL, Burkitt lymphoma; DH, double hit; DLBCL, diffuse large cell B-cell lymphoma.

neither myeloma cell line expressed high levels of IL6 (data not shown). In contrast, the mRNA levels of *IL6R* encoding CD126 or the IL6Rα subunit was significantly downregulated in MM1.S cells treated with INCB054329 at 4 hours [1.6-fold, false discovery rate (FDR) <0.002; Fig. 4C). A 2.4- to 3.5-fold reduction in *IL6R* mRNA within 4 hours was also observed in additional cell lines, including U-266, OPM-2, and KMS-11. Analysis of the gene track for BRD4 association with the IL*6R* gene locus showed strong enrichment near the TSS that corresponded to a peak of histone H3K27 acetylation in CD14-positive myeloid cells from project ENCODE data (Fig. 4D; ref. 22). This activation histone mark at the TSS was confirmed in MM1.S cells by ChIP-PCR for H3K27Ac (data not shown) and correlated with BRD4 association in control cells.

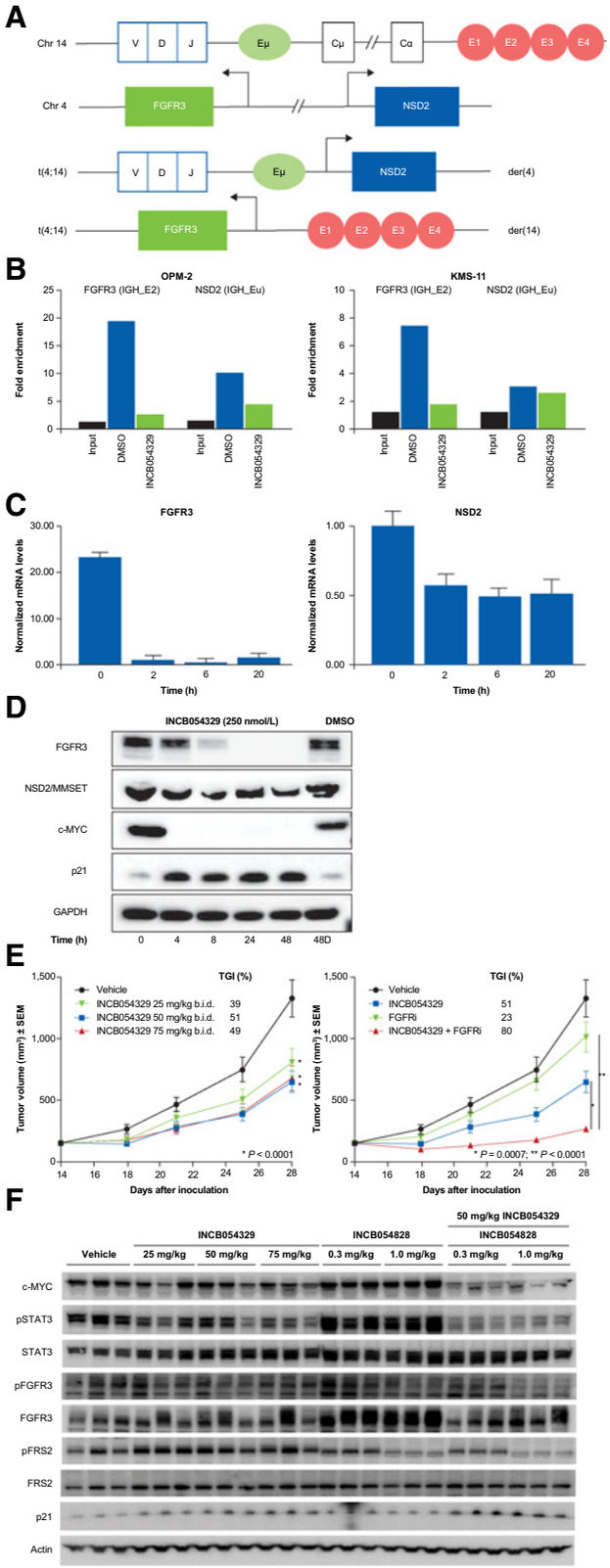

Treatment with JQ-1 abrogated the BRD4 peaks at this site. Similarly, treatment with INCB054329 resulted in depletion of BRD4 from the *IL6Rα* TSS in OPM-2 cells (Fig. 4E).

Suppression of IL6R by INCB054329 sensitizes myeloma cells to clinical Janus kinase (JAK) inhibitors

To evaluate whether the reduction of IL6Rα would translate into a vulnerability that could be therapeutically exploited, cellular analyses were performed to assess the effect on IL6Rα protein levels and signaling in myeloma cell lines. INCB054329 treatment induced a dose-dependent decrease in cell-surface IL6Rα staining as measured by flow cytometry in MM1.S and U-266 cells and in IL6Rα protein levels by Western blotting in MM1.S and U-266 cells that corresponded to decreased levels of IL6Rα protein (Fig. 5A). The consequence of IL6Rα reduction on IL6 signaling was measured in U-266 cells because they express high levels of IL6Rα but are not dependent on IL6 for survival, in contrast to INA-6 cells that rapidly lose viability upon loss of IL6 signaling (23). Basal levels of pSTAT3 were reduced by nearly eight fold with INCB054329 (Fig. 5B, compare lanes 1 to 4). Upon stimulation with IL6, a concentration-dependent increase in the pSTAT3 level was observed in both DMSO and INCB054329-treated groups; however, in cells pretreated with INCB054329, pSTAT3 was induced to an extent that only slightly exceeded the unstimulated DMSO control (Fig. 5B, compare lanes 1 and 6). Therefore, reducing cell-surface IL6Rα levels diminished the response to physiologically relevant levels of IL6. Consistent with this effect, transcriptional profiling showed decreased levels in expression of several genes also known to be at least in part transcriptionally regulated by STAT3, including BCL-xL, and cyclins D1 and D2 (Fig. 4C), indicating BET inhibition of IL6Rα levels results in decreased levels of several downstream pathway targets. As a possible compensatory response to suppressed IL6 signaling, genes in the IL6–JAK2–STAT3 pathway were upregulated, including time-dependent increases in JAK1, JAK2, STAT6, and STAT3 transcripts.

We reasoned that targeting of BET in combination with a selective JAK inhibitor could have combinatorial effects on myeloma cell viability, especially in view of potential compensatory increases in JAK–STAT pathway genes. Studies were

Figure 3.
INCB054329 reduces BRD4 binding to the IgH enhancer and reduces expression of target genes. **A,** Cartoon depicting the t(4;14)-balanced translocation resulting in fusion of the Eμ enhancer 3′ to *FGFR3* and the E2 enhancer 5′ to *NSD2* (13). **B,** ChIP-PCR analysis of BRD4 binding to the 3′ enhancer element E2 or the Eμ intronic enhancer in OPM-2 (left) or KMS-11 (right) cells treated with DMSO or INCB054329. Data are expressed as the fold enrichment normalized to the input (2% of DMSO sample). **C,** INCB054329 reduces expression of genes regulated by the IgH enhancer. Decrease in the steady-state levels of FGFR3 (left) and NSD2 (right) mRNA in OPM-2 cells treated with INCB054329 for 4 hours. **D,** Western blot analysis of bromodomain target proteins. OPM-2 cells were treated with 250 nmol/L of INCB054329, harvested over 48 hours, and analyzed for levels of the indicated proteins. The "0" indicates untreated cells, and "48D" are control cells treated for 48 hours with DMSO. **E,** Efficacy of INCB054329 in the OPM-2 subcutaneous xenograft model as monotherapy or in combination with the selective FGFR inhibitor INCB054828. **F,** Xenografted OPM-2 tumors were harvested from mice after 5 days of treatment with INCB054329 (50 mg/kg), INCB054828 (0.3 mg/kg), both agents, or vehicle, and Western blots of the indicated proteins were performed on the tumor lysates.

undertaken using the JAK1/2 inhibitor ruxolitinib (24) or the JAK1-selective inhibitor itacitinib (Supplementary Table S2). INA-6 cells were sensitive to both JAK and BET inhibitors, and combining either JAK inhibitor with INCB054329 potentiated the effect on viability. Using Bliss independence calculation (25), the average fractional product (Fua) across a 5 × 5

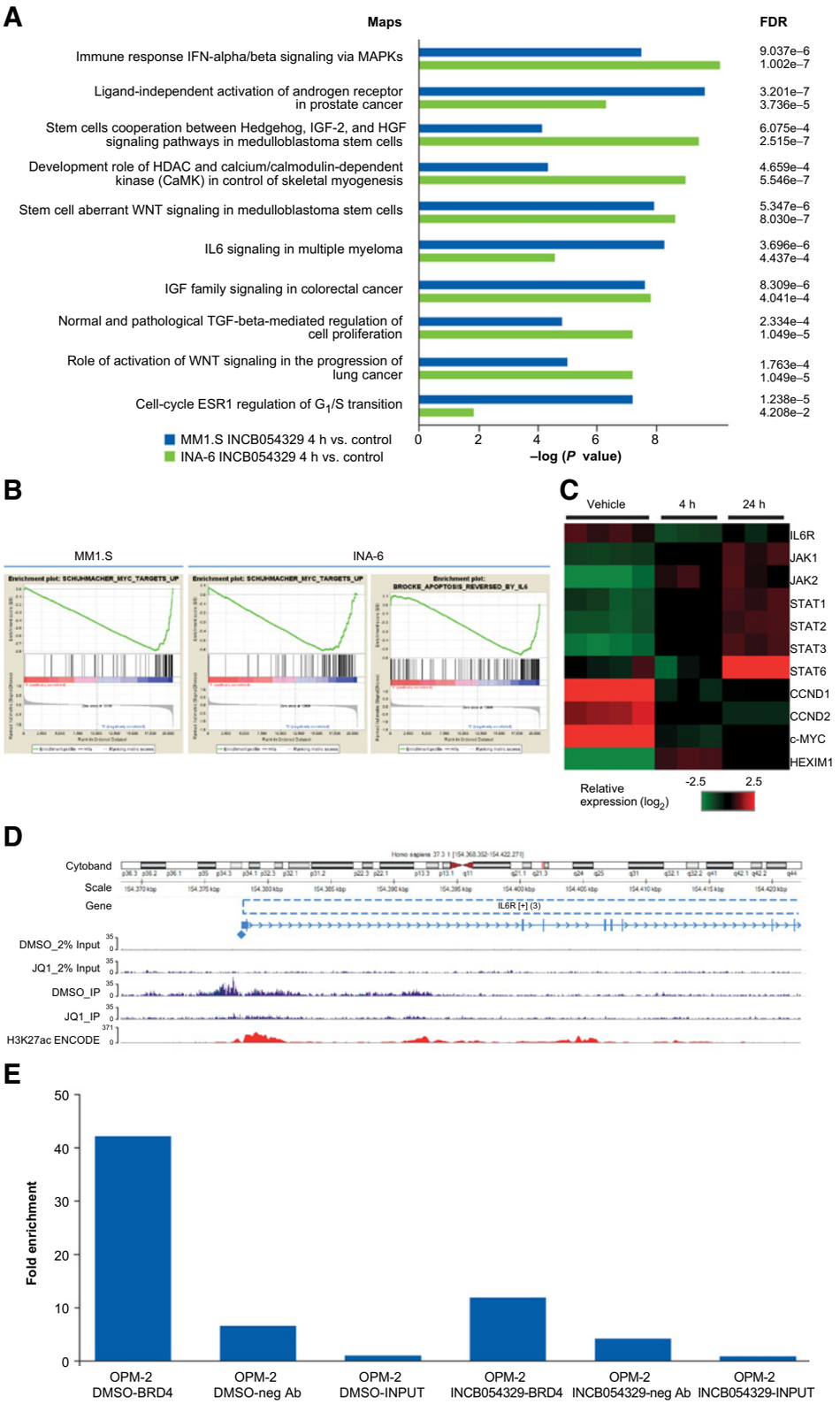

Figure 4.
Gene-expression profiling of myeloma cell lines treated with INCB054329 reveals regulation of pathways involved in growth, development, and inflammation. **A,** Top pathways identified using MetaCore in INA-6 cells and MM1.S cells treated with INCB054329 for 4 hours (genes used for pathway enrichment were selected by |Fold Change|>1.5 and FDR <0.05 in each cell line). **B,** Gene set enrichment analysis showing representative plots of gene sets strongly downregulated by treatment with INCB054329. **C,** Changes in expression of JAK–STAT pathway genes upon treatment with INCB054329 in MM1.S cells. **D,** BRD4 binding to the IL6Rα TSS is blocked by BET inhibitors. ChIP-sequencing reads of BRD4 in MM1.S cells treated with DMSO or 1 μmol/L of JQ-1. The gene track for H3K27 acetylation in CD14-positive cells from ENCODE consortium is shown for comparison (22). **E,** ChIP-PCR for BRD4 association with the TSS of IL6R in OPM-2 cells treated with 500 nmol/L of INCB054329 or DMSO using anti-BRD4 or a negative control antibody. Data are expressed as the fold enrichment normalized to the input (2% of DMSO sample).

combination grid was 7 and 12 for combinations with ruxolitinib and itacitinib, respectively, indicating a synergistic interaction. In contrast, a control grid of INCB054329 versus itself yielded an additive Fua of 1. The combination of either JAK inhibitor with INCB054329 also induced a greater degree of apoptosis (Fig. 5C). Analysis of downstream targets demonstrated that the combination of JAK1 and BET inhibitors had markedly enhanced inhibition of pSTAT3 and modestly greater

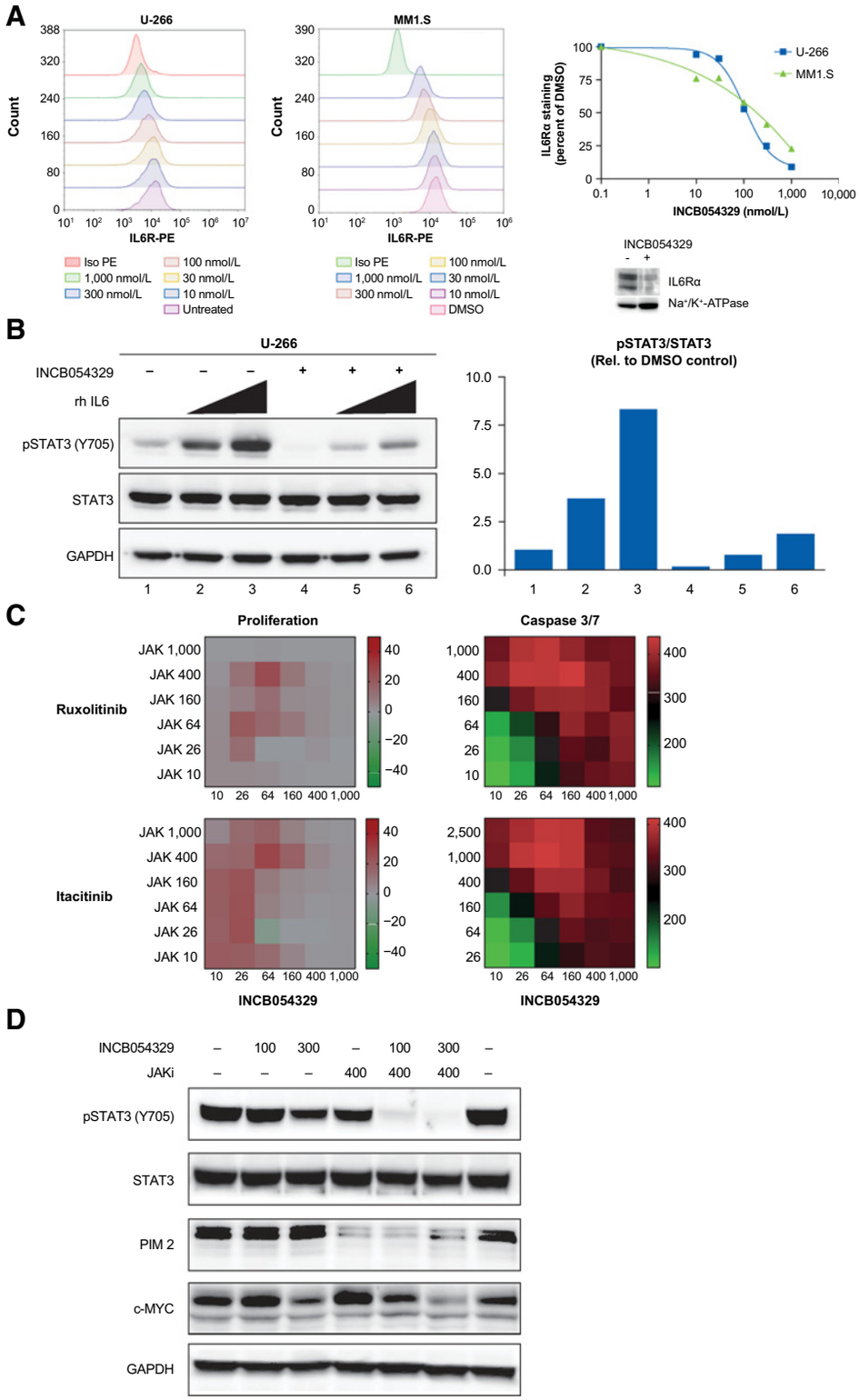

Figure 5.

INCB054329 suppression of IL6R reduces JAK–STAT signaling and sensitizes myeloma cells to combined inhibition with clinical JAK inhibitors. **A,** Concentration-dependent reduction of cell-surface IL6Rα in U-266 (left) or MM1.S cells (middle) treated for 48 hours with 10–1,000 nmol/L INCB054329. Right, the IC_{50} plots for reduction of cell-surface IL6Rα. Western blot analysis of IL6Rα protein and a membrane protein control (Na^+/K^+-ATPase) in cells treated with DMSO or 1 μmol/L of INCB054329 for 48 hours are shown. **B,** IL6-dependent signaling in U-266 cells treated with INCB054329 is diminished. Cells treated with DMSO or 500 nmol/L INCB054329 for 36 hours were stimulated with 0, 0.02, or 0.1 ng/mL of recombinant human IL6 for 10 minutes. Western blot analysis shows levels of phospho- and total STAT3 and GAPDH (left). Quantitation of the luminescence intensity of pSTAT3 normalized to total STAT3 and plotted relative to the unstimulated DMSO control sample (right). **C,** Heat maps (left) showing the Excess over Bliss values in INA-6 and MM1.S cells treated with a dilution series of INCB054329 and either ruxolitinib (top) or itacitinib (bottom) for 72 hours and assayed using CellTiter-Glo. Heat maps (right) showing the percent increase of caspase 3/7 activity in cells treated with a dilution series of INCB054329 and either ruxolitinib (top) or itacitinib (bottom) for 48 hours. **D,** Western blot analysis of INA-6 cells treated with INCB054329 (100 or 300 nmol/L), itacitinib (JAK inhibitor, 400 nmol/L), or the combination for 4 hours. Control cells were treated with DMSO. Iso, isotype antibody control; PE, phycoerythrin; rh, recombinant human.

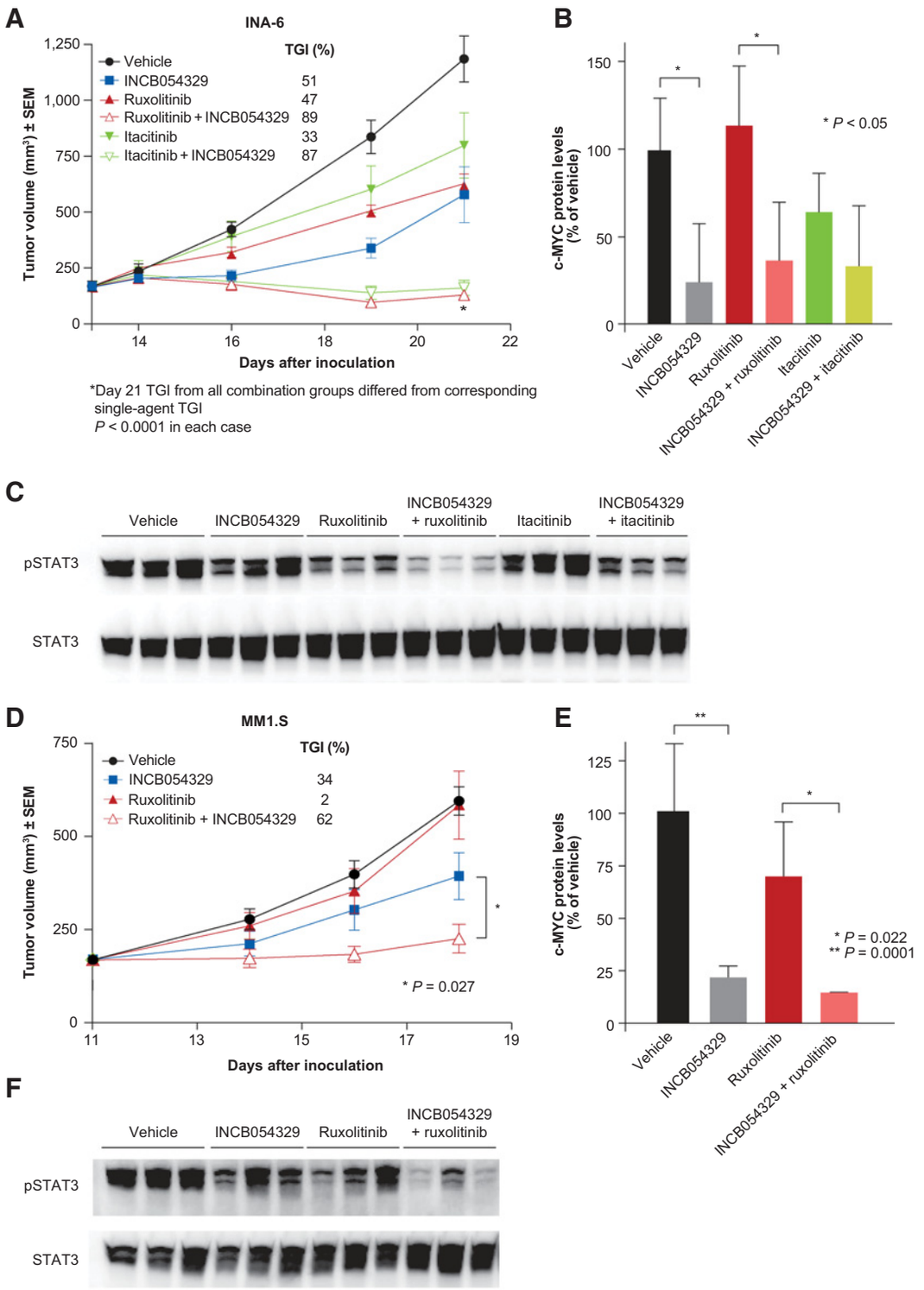

Figure 6.

Combination of BET and JAK inhibitors *in vivo* shows synergistic effects on tumor growth. **A,** Efficacy of INCB054329 and JAK inhibitor monotherapy or in combination in the subcutaneous INA-6 human myeloma xenograft model. **B,** Pharmacodynamic effects of INCB054329, JAK inhibitors, or the combination on c-MYC levels in INA-6 xenografted tumors following a single oral dose. **C,** Pharmacodynamic effects of INCB054329, JAK inhibitors, or the combination on pSTAT3 levels in INA-6 xenografted tumors following a single oral dose. **D,** Efficacy of INCB054329 and ruxolitinib monotherapy or in combination in the subcutaneous MM1.S human myeloma xenograft model. **E,** Pharmacodynamic effects of INCB054329, ruxolitinib, or the combination on c-MYC in MM1.S xenografted tumors following a single oral dose. **F,** Pharmacodynamic effects of INCB054329, ruxolitinib, or the combination on pSTAT3 in MM1.S xenografted tumors following a single oral dose.

suppression of c-MYC than either agent alone. Interestingly, JAK1 inhibition resulted in decreased protein levels of the STAT3 transcriptional target PIM2, whereas PIM2 levels remained unchanged by BET inhibition, suggesting that the BET and JAK1 inhibitors can differentially influence the outcome of STAT-mediated transcription (Fig. 5D). The MM1.S cell line that is independent of IL6 did not show sensitivity to any JAK inhibitor in viability assays nor did the addition of JAK inhibitor increase the activity of INCB054329 under standard culture conditions (data not shown).

Combination of JAK and BET inhibitors *in vivo* leads to enhanced efficacy

To evaluate whether the combination of JAK and BET inhibitors would translate to improved efficacy, INA-6 xenografts were established in female SCID mice. At a dose of 50 mg/kg b.i.d., INCB054329 reduced tumor growth by 51% ($P < 0.0001$, two-way ANOVA) compared with the vehicle control group after 8 days of oral dosing (Fig. 6A). A dose of ruxolitinib suitable for combination studies (30 mg/kg b.i.d.) also suppressed tumor growth by 47% ($P < 0.0001$). The combination of ruxolitinib and INCB054329 significantly enhanced the efficacy (89% tumor growth inhibition) and resulted in partial tumor regressions in five of eight animals. The combinations with itacitinib at a dose of 60 mg/kg b.i.d. exhibited similar results, with each combination significantly reducing tumor size when compared with its single-agent arms ($P < 0.0001$, two-way ANOVA for each). All combinations were well tolerated based on body-weight measurements.

The pharmacodynamic effects of the BET and JAK inhibitors were also examined in the INA-6 xenograft model. Levels of c-MYC protein were lower in tumors from INCB054329-treated mice than vehicle controls (Fig. 6B). Levels of pSTAT3 were decreased by ruxolitinib alone, and the combination of the BET inhibitor with either JAK inhibitor further decreased STAT3 phosphorylation (Fig. 6C), consistent with the results *in vitro*.

The combination of INCB054329 with ruxolitinib was also tested in the IL6-independent model MM1.S. Similar to the *in vitro* data, subcutaneous xenografts of the MM1.S tumor were insensitive to ruxolitinib monotherapy (Fig. 6D) at the same dose (30 mg/kg b.i.d.) used in the INA-6 study. Surprisingly, despite this lack of effect with ruxolitinib, tumor growth was suppressed to a significantly greater extent by INCB054329 in combination with ruxolitinib compared with the BET inhibitor alone ($P < 0.05$, two-way ANOVA for combination vs. either single agent). INCB054329 significantly decreased tumor c-MYC levels (Fig. 6E), and levels of pSTAT3 were partially reduced by either BET or JAK inhibition and showed further reduction in the combination groups (Fig. 6F).

Discussion

Here, we present an extensive preclinical characterization of INCB054329, a structurally distinct and rationally designed BET inhibitor that has been evaluated in phase I clinical trials (NCT02431260). INCB054329 potently and selectively antagonizes the BET subfamily of bromodomain proteins and shows antiproliferative activity against cancer cell lines derived from hematologic malignancies of different histologies. Treatment with INCB054329 reduced c-MYC levels in cell lines as well as in subcutaneous xenograft tumors, with an *in vivo* IC_{50} value of 66 nmol/L and maximally reduced c-MYC with a plasma concentration of 399 nmol/L. Using these data, the maximum efficacy of single-agent therapy was observed when the *in vivo* IC_{50} was exceeded for at least 14 hours, which was achieved by twice-daily administration.

Previous studies have shown antimyeloma activity of BET inhibitors by downregulation of oncogenic signaling through c-MYC (13, 19, 26). In addition to these well-characterized effects, BET inhibitors also diminish bromodomain protein binding to the IgH enhancer in the 14q32 translocation setting, including the t(8;14) translocation (involving 14q32) linking IgH to *MYC*. Although the t(8;14) translocation is present only in a very small percentage of patients with multiple myeloma, several other reciprocal translocations involving 14q32 lead to highly increased levels of oncogenic proteins, most prominently MAF, CCND1, CCND3, and MMSET/FGFR3 (11, 12). Oncogene upregulation by IgH drives distinct gene-expression signatures that can be used to categorize myelomas into subgroups (27). The utility of BET inhibition in myeloma becomes more apparent due to the ability of BET proteins to target downstream growth-promoting effectors such as growth factors and cytokines that are expressed across myeloma subgroups. Likewise, BET inhibition may also be effective regardless of subgroup or genetic alteration due to its ability to block transcriptional activity from the IgH locus.

Among the most prevalent alteration is the t(4;14)-balanced translocation, in which the intronic Eμ enhancer is joined to NSD2 on der4 while the 3′ enhancers segregate with FGFR3 on der14 (13). BRD4 binding was detected at both enhancer elements in t(4;14)-positive cell lines, but the dependence upon BRD4 was not equivalent. Inhibition by INCB054329 resulted in a dramatic decrease in FGFR3 expression and protein, while levels of NSD2 were only modestly affected. In cell lines that have a partial dependency on FGFR3 signaling for survival, the depletion of FGFR3 created a vulnerability that could be exploited by combination with selective FGFR-targeted inhibitors. *In vivo*, combination of INCB054329 with the selective FGFR1/2/3 inhibitor INCB054828 showed significantly greater efficacy than either mechanism alone. A strong feedback signal resulted from FGFR targeting that may have limited the efficacy of FGFR inhibitor monotherapy. Importantly, this adaptive response was completely abrogated by combination with INCB054329. The idea of combining signaling pathway inhibitors with BET inhibitors to decrease expression of genes within the pathway and to counter feedback activation is a potentially powerful strategy. Indeed, this concept has been previously validated for combinations of BET inhibitors with the Bruton tyrosine kinase inhibitor ibrutinib in models of non-Hodgkin lymphoma (28, 29), and with phosphoinositide 3-kinase or epidermal growth factor receptor 1/2 kinase inhibitors in models of breast cancer and other solid tumors (30, 31).

In addition to direct regulation of oncogenes, BET inhibition can regulate levels of effectors downstream of the oncogenic signal. For example, BET proteins have been shown to regulate expression of proinflammatory genes including cytokines, chemokines, and their receptors in models of acute inflammation (8, 10). Gene-expression profiling revealed that immune and inflammatory pathways were strongly enriched by treatment of myeloma cell lines with INCB054329, even in the absence of acute challenge. Notably, *IL6R* has been found to be strongly overexpressed across several multiple myeloma subgroups (27). *IL6R* is a direct target of BRD4, and inhibition by INCB054329 or

JQ-1 displaced it from the *IL6R* TSS suppressing the expression of IL6Rα and resulting in diminished signaling through STAT3 even upon IL6 stimulation. An apparent compensatory response to decreased IL6–JAK–STAT signaling was evidenced by upregulation of components of the JAK–STAT signaling pathway. Consistent with this finding, combinations with the clinical JAK inhibitors ruxolitinib or itacitinib further reduced JAK–STAT signaling in the IL6-dependent INA-6 model, resulting in synergistic inhibition of proliferation and enhanced apoptosis in cells. Combining BET and JAK inhibitors resulted in superior efficacy at well-tolerated doses and together suppressed levels of pSTAT3 more effectively than either agent alone. The importance of IL6 as a growth and survival factor for myeloma cells and as a modulator of cellular interactions in the myeloma tumor microenvironment is well documented (11, 32). Gene-expression analysis of human myeloma has revealed a significant subset of tumors with an activated STAT signature (33). In murine models, activated IL6–JAK–STAT signaling and c-MYC have been shown to collaborate in the development of myeloma. An intercross of mice harboring a human IL6 transgene with Eμ-c-MYC mice resulted in the acceleration of plasma cell tumor formation with full penetrance (34). Separately, a murine transduction–transplantation model of myeloma driven by a constitutively active allele of Gp130 encoding the common coreceptor subunit for cytokine receptors, including IL6Rα, also showed enhanced tumorigenesis in cooperation with c-MYC. In plasmacytomas arising from Gp130 activation alone, activating genetic alterations in the c-MYC locus were recovered in three of ten independently arising tumors (33). Combining JAK and BET inhibitors is a potentially promising strategy for other hematologic malignancies, including JAK2V617-dependent myeloproliferative neoplasms and acute lymphocytic leukemia (ALL) characterized by IL7R activation (35–38). In the ALL models, JQ-1 suppressed STAT5-dependent signaling and improved survival; significantly at relapse, these tumors showed reactivation of STAT5 signaling indicating a feedback upregulation of JAK–STAT signaling.

The mechanism for synergy merits additional study and should consider both cell-intrinsic and cell-extrinsic mechanisms given that BET inhibitors may affect expression of soluble mediators within the tumor microenvironment that may be important for supporting tumor cell viability. As an example, the MM1.S xenograft model, which does not respond to JAK inhibition alone, was unexpectedly sensitized to JAK inhibition by coadministration of INCB054329 *in vivo*. This sensitivity to combined JAK and BET inhibition was not observed *in vitro*. One potential explanation for these findings is that the levels of cytokines or growth factors in the tumor microenvironment that provide protection from JAK inhibition may not be as high as those in cell culture. It is also possible that BET inhibition could make some myelomas more reliant on cytokine signaling for survival, consistent with the upregulation of JAK–STAT pathway genes. Finally, it is possible that BET inhibitors have biological effects on other cell types within the tumor microenvironment that may support the malignant cells. Preliminary data show that BET inhibition can markedly reduce the secretion of multiple cytokines, including IL6 and IL8 (Supplementary Fig. S5), in cultured stromal cell lines at concentrations below the IC_{50} for suppression of cell growth. Thus, *in vivo* BET inhibition may have pleiotropic biological impacts beyond direct effects on the malignant clone.

In summary, we present the profile of a BET inhibitor, INCB054329, that has advanced into phase I trials. Using myeloma as a model, we identified oncogenes and inflammatory pathways regulated by BET proteins that are significantly altered by treatment with the INCB054329. Preliminary clinical data from trials with BET inhibitors have shown only modest single-agent efficacy to date in hematologic cancers, including myeloma, suggesting that rational therapeutic combinations designed to target different aspects of cancer biology may be required to enhance responses in patients with advanced malignancies (39). By evaluating BET inhibitor–induced changes in growth-promoting and survival pathways, vulnerabilities are revealed that can guide rational combinations such as with FGFR inhibitors in the case of selected t(4;14)-rearranged myelomas and with JAK inhibitors in models characterized by an enriched IL6 signature. Importantly, the effects of INCB054329 on these targets were achieved using modest concentrations (approximately 2–3 × *in vivo* IC_{50}), suggesting that these findings can be translatable to the clinic. By targeting different aspects of tumor biology, combination therapy may overcome the tumor heterogeneity and complexity that may be contributing to limited single-agent efficacy in early trials.

Disclosure of Potential Conflicts of Interest

M.C. Stubbs, T.C. Burn, A. Volgina, N. Zolotarjova, J. Li, R. Collins, V. Dostalik, R. Wynn, B. Ruggeri, S. Yeleswaram, R. Huber, and P.C.C. Liu have ownership interests (including patents) in Incyte Corporation. No potential conflicts of interest were disclosed by the other authors.

Authors' Contributions

Conception and design: M.C. Stubbs, T.C. Burn, T. Maduskuie, R. Wynn, W. Yao, A.P. Combs, R. Huber, G. Hollis, P. Scherle, P.C.C. Liu
Development of methodology: M.C. Stubbs, T.C. Burn, A. Volgina, N. Zolotarjova, M. Favata, X.M. Liu, J. Li, N. Falahatpisheh, P. Polam, P. Thekkat, X. He, M. Covington
Acquisition of data (provided animals, acquired and managed patients, provided facilities, etc.): M. Rupar, X. Wen, N. Zolotarjova, M. Favata, X.M. Liu, J. Li, D. DiMatteo, P. Feldman, P. Thekkat, C. Gardiner, Y. Li, M. Covington, R. Wynn, P.C.C. Liu
Analysis and interpretation of data (e.g., statistical analysis, biostatistics, computational analysis): M.C. Stubbs, T.C. Burn, S. Diamond, M. Rupar, A. Volgina, N. Zolotarjova, M. Favata, H. Liu, X.M. Liu, J. Li, P. Feldman, P. Thekkat, C. Gardiner, X. He, M. Covington, R. Wynn, S. Yeleswaram, P. Scherle, P.C.C. Liu
Writing, review, and/or revision of the manuscript: M.C. Stubbs, T.C. Burn, M. Rupar, R. Collins, V. Dostalik, M. Covington, B. Ruggeri, G. Hollis, P. Scherle, P.C.C. Liu
Administrative, technical, or material support (i.e., reporting or organizing data, constructing databases): B. Ruggeri
Study supervision: M.C. Stubbs, S. Diamond, B. Ruggeri, S. Yeleswaram, C.-B. Xue, R. Huber, P.C.C. Liu
Other (medicinal chemistry research): R. Sparks
Other (contributing author): P. Waeltz
Other (research: Molecular modeling): R. Jalluri

Acknowledgments

Medical writing assistance was provided by Abigail Marmont of Evidence Scientific Solutions Inc., Wilmslow, UK, and funded by Incyte Corporation.

The costs of publication of this article were defrayed in part by the payment of page charges. This article must therefore be hereby marked *advertisement* in accordance with 18 U.S.C. Section 1734 solely to indicate this fact.

Received February 8, 2018; revised June 20, 2018; accepted September 7, 2018; published first September 11, 2018.

References

1. Filippakopoulos P, Knapp S. Targeting bromodomains: epigenetic readers of lysine acetylation. Nat Rev Drug Discov 2014;13: 337–56.
2. Shi J, Vakoc CR. The mechanisms behind the therapeutic activity of BET bromodomain inhibition. Mol Cell 2014;54:728–36.
3. Hnisz D, Abraham BJ, Lee TI, Lau A, Saint-André V, Sigova AA, et al. Super-enhancers in the control of cell identity and disease. Cell 2013; 155:934–47.
4. Lovén J, Hoke HA, Lin CY, Lau A, Orlando DA, Vakoc CR, et al. Selective inhibition of tumor oncogenes by disruption of super-enhancers. Cell 2013;153:320–34.
5. Mochizuki K, Nishiyama A, Jang MK, Dey A, Ghosh A, Tamura T, et al. The bromodomain protein Brd4 stimulates G1 gene transcription and promotes progression to S phase. J Biol Chem 2008;283: 9040–8.
6. Yang Z, He N, Zhou Q. Brd4 recruits P-TEFb to chromosomes at late mitosis to promote G1 gene expression and cell cycle progression. Mol Cell Biol 2008;28:967–76.
7. Filippakopoulos P, Qi J, Picaud S, Shen Y, Smith WB, Fedorov O, et al. Selective inhibition of BET bromodomains. Nature 2010;468: 1067–73.
8. Nicodeme E, Jeffrey KL, Schaefer U, Beinke S, Dewell S, Chung CW, et al. Suppression of inflammation by a synthetic histone mimic. Nature 2010;468:1119–23.
9. Zuber J, Shi J, Wang E, Rappaport AR, Herrmann H, Sison EA, et al. RNAi screen identifies Brd4 as a therapeutic target in acute myeloid leukaemia. Nature 2008;478:524–8.
10. Belkina AC, Nikolajczyk BS, Denis GV. BET protein function is required for inflammation: Brd2 genetic disruption and BET inhibitor JQ1 impair mouse macrophage inflammatory responses. J Immunol 2013;190: 3670–8.
11. Anderson KC, Carrasco RD. Pathogenesis of myeloma. Annu Rev Pathol 2011;6:249–74.
12. Kuehl WM, Bergsagel PL. Molecular pathogenesis of multiple myeloma and its premalignant precursor. J Clin Invest 2012;122: 3456–63.
13. Chesi M, Nardini E, Lim RS, Smith KD, Kuehl WM, Bergsagel PL. The t(4;14) translocation in myeloma dysregulates both FGFR3 and a novel gene, MMSET, resulting in IgH/MMSET hybrid transcripts. Blood 1998; 92:3025–34.
14. Affer M, Chesi M, Chen WG, Keats JJ, Demchenko YN, Roschke AV, et al. Promiscuous MYC locus rearrangements hijack enhancers but mostly super-enhancers to dysregulate MYC expression in multiple myeloma. Leukemia 2014;28:1725–35.
15. Walker BA, Wardell CP, Brioli A, Boyle E, Kaiser MF, Begum DB, et al. Translocations at 8q24 juxtapose MYC with genes that harbor super-enhancers resulting in overexpression and poor prognosis in myeloma patients. Blood Cancer J 2014;4:e191.
16. Kawano Y, Moschetta M, Manier S, Glavey S, Gorgun GT, Roccaro AM, et al. Targeting the bone marrow microenvironment in multiple myeloma. Immunol Rev 2015;263:160–72.
17. Mootha VK, Lindgren CM, Eriksson KF, Subramanian A, Sihag S, Lehar J, et al. PGC-1alpha-responsive genes involved in oxidative phosphorylation are coordinately downregulated in human diabetes. Nat Genet 2003;34: 267–73.
18. Subramanian A, Tamayo P, Mootha VK, Mukherjee S, Ebert BL, Gillette MA, et al. Gene set enrichment analysis: a knowledge-based approach for interpreting genome-wide expression profiles. Proc Natl Acad Sci U S A 2005;102:15545–50.
19. Delmore JE, Issa GC, Lemieux ME, Rahl PB, Shi J, Jacobs HM, et al. BET bromodomain inhibition as a therapeutic strategy to target c-Myc. Cell 2011;146:904–17.
20. Holien T, Vatsveen TK, Hella H, Waage A, Sundan A. Addiction to c-MYC in multiple myeloma. Blood 2012;120:2450–3.
21. Mertz JA, Conery AR, Bryant BM, Sandy P, Balasubramanian S, Mele DA, et al. Targeting MYC dependence in cancer by inhibiting BET bromodomains. Proc Natl Acad Sci U S A 2011;108:16669–74.
22. Dunham I, ENCODE Project Consortium. An integrated encyclopedia of DNA elements in the human genome. Nature 2012;489:57–74.
23. Burger R, Guenther A, Bakker F, Schmalzing M, Bernand S, Baum W, et al. Gp130 and ras mediated signaling in human plasma cell line INA-6: a cytokine-regulated tumor model for plasmacytoma. Hematol J 2001;2:42–53.
24. Quintás-Cardama A, Vaddi K, Liu P, Manshouri T, Li J, Scherle PA, et al. Preclinical characterization of the selective JAK1/2 inhibitor INCB018424: therapeutic implications for the treatment of myeloproliferative neoplasms. Blood 2010;115:3109–17.
25. Foucquier J, Guedj M. Analysis of drug combinations: current methodological landscape. Pharmacol Res Perspect 2015;3:e00149.
26. Chaidos A, Caputo V, Gouvedenou K, Liu B, Marigo I, Chaudhry MS, et al. Potent antimyeloma activity of the novel bromodomain inhibitors I-BET151 and I-BET762. Blood 2014;123:697–705.
27. Zhan F, Huang Y, Colla S, Stewart JP, Hanamura I, Gupta S, et al. The molecular classification of multiple myeloma. Blood 2006;108: 2020–8.
28. Ceribelli M, Kelly PN, Shaffer AL, Wright GW, Xiao W, Yang Y, et al. Blockade of oncogenic IκB kinase activity in diffuse large B-cell lymphoma by bromodomain and extraterminal domain protein inhibitors. Proc Natl Acad Sci U S A 2014;111:11365–70.
29. Sun B, Shah B, Fiskus W, Qi J, Rajapakshe K, Coarfa C, et al. Synergistic activity of BET protein antagonist-based combinations in mantle cell lymphoma cells sensitive or resistant to ibrutinib. Blood 2015;126: 1565–74.
30. Stratikopoulos EE, Dendy M, Szabolcs M, Khaykin AJ, Lefebvre C, Zhou MM, et al. Kinase and BET inhibitors together clamp inhibition of PI3K signaling and overcome resistance to therapy. Cancer Cell 2015; 27:837–51.
31. Stuhlmiller TJ, Miller SM, Zawistowski JS, Nakamura K, Beltran AS, Duncan JS, et al. Inhibition of lapatinib-induced kinome reprogramming in ERBB2-positive breast cancer by targeting BET family bromodomains. Cell Rep 2015;11:390–404.
32. Rosean TR, Tompkins VS, Tricot G, Holman CJ, Olivier AK, Zhan F, et al. Preclinical validation of interleukin 6 as a therapeutic target in multiple myeloma. Immunol Res 2014;59:188–202.
33. Dechow T, Steidle S, Gotze KS, Rudelius M, Behnke K, Pechloff K, et al. GP130 activation induces myeloma and collaborates with MYC. J Clin Invest 2014;124:5263–74.
34. Rutsch S, Neppalli VT, Shin DM, DuBois W, Morse HC 3rd,Goldschmidt H, et al. IL-6 and MYC collaborate in plasma cell tumor formation in mice. Blood 2010;115:1746–54.
35. Saenz DT, Fiskus W, Manshouri T, Rajapakshe K, Krieger S, Sun B, et al. BET protein bromodomain inhibitor-based combinations are highly active against post-myeloproliferative neoplasm secondary AML cells. Leukemia 2017;31:678–87.
36. Wyspianska BS, Bannister AJ, Barbieri I, Nangalia J, Godfrey A, Calero-Nieto FJ, et al. BET protein inhibition shows efficacy against JAK2V617F-driven neoplasms. Leukemia 2014;28:88–97.
37. Ott CJ, Kopp N, Bird L, Paranal RM, Qi J, Bowman T, et al. BET bromodomain inhibition targets both c-Myc and IL7R in high-risk acute lymphoblastic leukemia. Blood 2012;120:2843–52.
38. Kleppe M, Koche R, Zou L, van Galen P, Hill CE, Dong L, et al. Dual targeting of oncogenic activation and inflammatory signaling increases therapeutic efficacy in myeloproliferative neoplasms. Cancer Cell 2018; 33:29–43 e7.
39. Amorim S, Stathis A, Gleeson M, Iyengar S, Magarotto V, Leleu X, et al. Bromodomain inhibitor OTX015 in patients with lymphoma or multiple myeloma: a dose-escalation, open-label, pharmacokinetic, phase 1 study. Lancet Haematol 2016;3:e196–204.